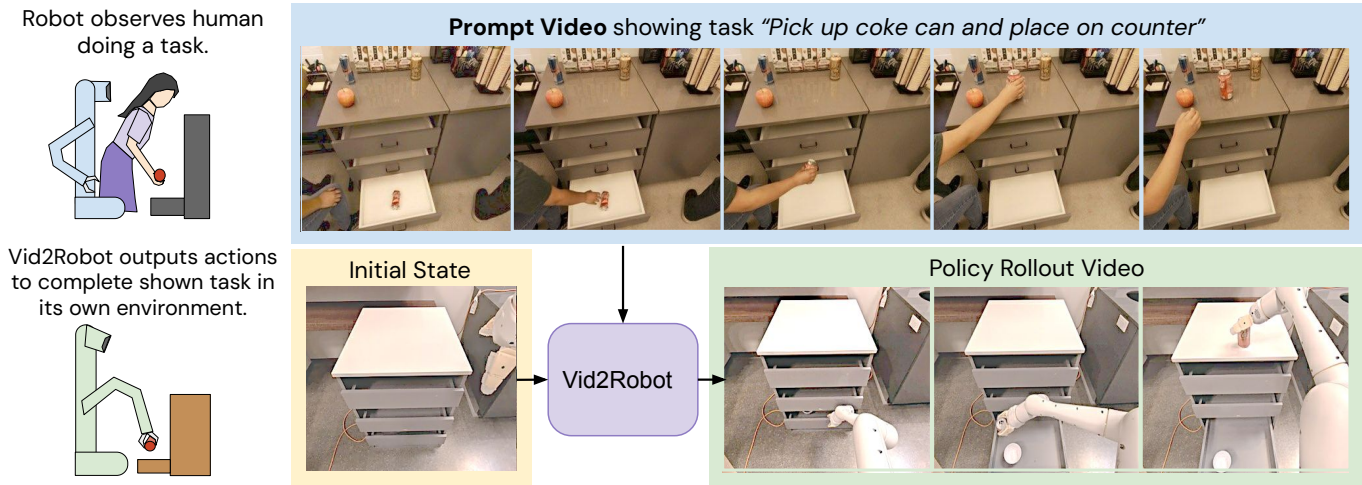


# Vid2Robot: End-to-end Video-conditioned Policy Learning with Cross-Attention Transformers

Vidhi Jain<sup>1,2</sup> Maria Attarian<sup>1,3</sup> Nikhil J Joshi<sup>1</sup> Ayzaan Wahid<sup>1</sup> Danny Driess<sup>1</sup> Quan Vuong<sup>1</sup> Pannag R Sanketi<sup>1</sup>  
Pierre Sermanet<sup>1</sup> Stefan Welker<sup>1</sup> Christine Chan<sup>1</sup> Igor Gilitschenski<sup>3</sup> Yonatan Bisk<sup>2</sup> Debidatta Dwibedi<sup>1</sup>

<sup>1</sup>Google DeepMind Robotics <sup>2</sup>Carnegie Mellon University <sup>3</sup>University of Toronto

arXiv:2403.12943v2 [cs.RO] 27 Aug 2024



**Fig. 1: Overview.** Vid2Robot is a video-conditioned robot policy. Given a human demonstration (top), Vid2Robot recognizes the task semantics and performs the same task based on the robot’s current visual observation (bottom left). A successful trajectory is presented on the bottom right.

**Abstract**—Large-scale multi-task robotic manipulation systems often rely on text to specify the task. In this work, we explore whether a robot can learn by observing humans. To do so, the robot must understand a person’s intent and perform the inferred task despite differences in the embodiments and environments. We introduce Vid2Robot, an end-to-end video-conditioned policy that takes human videos demonstrating manipulation tasks as input and produces robot actions. Our model is trained with a large dataset of prompt video-robot trajectory pairs to learn unified representations of human and robot actions from videos. Vid2Robot uses cross-attention transformer layers between video features and the current robot state to produce the actions and perform the same task as shown in the video. We use auxiliary contrastive losses to align the prompt and robot video representations for better policies. We evaluate Vid2Robot on real-world robots and observe over 20% improvement over BC-Z when using human prompt videos. Further, we also show cross-object motion transfer ability that enables video-conditioned policies to transfer a motion observed on one object in the prompt video to another object in the robot’s own environment. Videos available at [vid2robot.github.io](https://vid2robot.github.io).

## I. INTRODUCTION

The path to creating versatile robots that assist in people’s daily routines requires them to learn new skills on-the-go. These skills can vary from simple preferences for arranging dishes in the dishwasher in a specific household to completely different approaches to household cleaning. Humans can communicate in natural language for tasks that are already

known. However, we revert to demonstrations when we want to learn a novel skill with nuance. For example, we might show how a particular microwave works or how to organize our cabinets. Robots need the same ability for generalization from demonstration, which comes so naturally to humans.

Humans can infer the intentions of other humans based on third-person visual observations. Often, we use social reasoning and common sense to understand others’ goals implicitly. This ability is crucial for learning everyday tasks, such as kneading dough or knitting, where the intricacies are challenging to convey through still images or text [6]. We often turn to How-To videos [32]) to learn how to perform such tasks. If robots could act based on videos, it would enable efficient task learning and improved interaction with humans.

This work focuses on visual imitation learning, where robots learn to perform tasks by watching video demonstrations. This setup offers several advantages. First, it allows robots to learn from agents with a different embodiment, enabling new skill acquisition without teleoperation. Second, it allows robots to infer tasks from expert demonstrations, even if the expert is not showing how to perform tasks in the same environment as the robot. Finally, visual imitation learning is ideal for teaching tasks that are difficult or impossible to describe in words.

Existing multi-task robot manipulation models (e.g. RT-1 [8], RT-2 [9], and RT-X [35]) use language conditioning to output a robot trajectory. Relying on text alone for task spec-

ification makes it difficult for robots to handle polysemy and tasks whose executions vary dramatically based on context. For example, ‘open drawer’, ‘open cabinet’, ‘open container with lid’ and ‘open jar with screw cap’ might share the same verb but require very different motor control for each interaction. Here, the agent should not generalize its policy, whereas it should generalize from one *drawer* to others that vary in type, color, and shape. For this reason, there are a broad range of tasks for which it is hard to design primitives for high-level planning approaches [27, 2].

Another common approach has been to use a final goal image in goal-conditioned behavior cloning tasks [33, 25]. However, *how* to act is often ignored in such specifications. For example, ‘hold the flag’ and ‘wave the flag’ can have the same final goal image. We can resolve this ambiguity by using several sub-goal frames, that is quite close to conditioning robot policies with videos.

Current success of video conditioned policies in [42] assume that the provided video is from the same workspace with limited variability. Video-conditioned policies also lag in performance compared to language-conditioned policies work [22]. Based on these and related work, we identify three main challenges for video-conditioned policies: (1) Raw videos are high dimensional data that require more computational power and memory. (2) While unlabeled video data are abundant on the internet, finding robot-specific video and motion data is hard. (3) People can perform the same task differently due to variations in objects, lighting conditions, and other background distractions.

Despite these challenges, video-conditioned policy learning is a core challenge robots need to master. To this end, we study how end-to-end models with video-conditioning can be used to specify tasks to the robot. Vid2Robot is an end-to-end system that enables rapid adaptation to tasks specified as video demonstrations. Unlike prior work that either learned representations from videos for only object and verb recognition [22] or learned motor control in simulation [47], our work demonstrates the applicability of end-to-end learned video representations for real-world robotic control.

We present the key contributions of our work as follows: (1) We present a transformer-based policy to encode video task specification, demonstrated by either robot or human agent embodiments (§II). (2) We encourage alignment between the prompt and robot video representations using three contrastive auxiliary losses during training (§II-E) (3) Through actual robot experiments, we find our video-conditioned policy is better than baselines on human prompt videos. Furthermore, our policy is better at cross-object motion transfer (§III).

## II. APPROACH

### A. Preliminaries

Our objective is to design a robotic system that takes in a *prompt video* of a manipulation task and outputs actions that accomplish the task demonstrated in the video. This system must infer the underlying task from the prompt video (which might have a different setup or embodiment than the robot)

and then manipulate the objects in its environment to achieve the inferred task. Our model’s inputs are a prompt video  $V$  and the robot state  $S_t = \{x_i\}_{i=t-k}^t$  where  $x_i$  is the frame from the robot’s camera stream at time  $i$ ,  $k$  is the maximum number of historical frames, and  $t$  is the current timestep We train a policy  $\pi(a_t|S_t, V)$  that infers the underlying task from  $V$  and predicts task-relevant action  $a_t$ . We need a dataset of paired prompt videos and robot trajectories to train this model. Below, we will discuss in detail how to create paired datasets.

### B. Datasets

We need a dataset of pairs to train a video-conditioned robot policy: prompt videos and robot trajectories that perform the same task. In this work, we explore prompt videos where humans and robots perform the task. To create this dataset, we rely on three classes of data:







(1) *Robot-Robot*: We pair existing robot-robot videos of the same task. For this pairing, we consider two videos to *match* if they perform the same task in different settings. We define “*task*” based on natural language instructions for recording robot trajectories. These instructions typically consist of one or two verbs surrounded by nouns, such as ‘*place* water bottle upright’, ‘*move* the coke can to the green chip bag’ or ‘*open* top drawer’. Note that we use language instructions only for pairing and as an input to the robot policy. The objective of this pairing is two-fold: first, to leverage the already labeled and collected dataset of robot trajectories, and second, to ensure robots can imitate the same task but in different environment.

(2) *Hindsight Human-Robot*: Here, we use the task instructions from the robot trajectories dataset, ask one to five human participants to perform the task, and record a demonstration video from the robot’s perspective/view. The instructions are the same as before, but there is a significant embodiment and speed variability due to different humans performing the task with left or right hands and at a randomized robot camera angle. This provides us with a lot of paired data for training the policy with the available set of instructions in the robot dataset, without having to collect new robot trajectories.

(3) *Co-located Human-Robot*: In this case, humans and robots perform the same task in the same workspace. We used this approach to collect human demonstrations and robot trajectories in diverse spaces such as a living space with sofas, a meeting room with whiteboards, a hardware workstations with toy tools, a kitchen with countertop, a refrigerator and a sink, a storage supplies area, and more.

We show examples of paired videos of the prompt and robot demo from each of the three datasets in Figure 2. As can be seen, there is a considerable difference in the backgrounds and distractor objects in the Hindsight Human-Robot and Co-located Human-Robot datasets. A different complexity arises when comparing the first approach (Robot-Robot), where the actor is a robot with the same morphology, to the other two cases where the human is the actor in the prompt videos.

Each source represents a different level of difficulty and time to collect. Pairing existing robot datasets requires no extra data collection but does not involve any human demonstrations. Our

| Dataset Name           | Prompt Video Embodiment | Prompt v/s Robot Scene | Prompt Video  | Robot Video  |
|------------------------|-------------------------|------------------------|---|--|
| Robot-Robot            | Robot                   | Different              |  |  |
| Hindsight Human-Robot  | Human                   | Different              |  |  |
| Co-located Human-Robot | Human                   | Same                   |  |  |

**Fig. 2: Dataset creation.** (top row) Here we show a Robot-Robot video pair for *placing the rxbar into top drawer*. We similarly pair existing robot-robot videos performing the same task. (middle row) Here, we show Hindsight Human-Robot paired videos for *picking a Coke can from the bottom drawer and placing it on the counter* task. We use the task instructions from robot trajectories, ask human participants to perform the task and record a demonstration video from the robot’s perspective/view. (bottom row) Here, we show a Co-located Human-Robot pair of videos for *placing the pipe wrench in the toolkit*. We record a human demonstration and a robot teleoperation in the same workspace. We use different workspaces to perform the same task instruction, thus collecting paired videos with visually diverse prompts and robot state observations. More details in Section II-B.

second data involves asking humans to mimic existing robot trajectories. Hindsight human videos made data collection easier as they do not need robot teleoperation data. However, this did not increase the diversity of tasks in the data set. Lastly, we collect data with humans and robots in the same environment. While collecting co-located paired data is a presumed gold standard, it is very time and labor-intensive compared to the previous two approaches. Thus, it forms a small fraction of our overall training set. After combining all the datasets, we have  $\sim 100k$  robot videos and  $\sim 10k$  human videos covering the tasks introduced in RT-1 [8] and RT-2 [9]. The robot-robot dataset makes up more than 90% of the entire dataset. This dataset is publicly available [35]. We provide a Python Notebook in Supplementary Material for accessible visualization of the paired videos used in training.

### C. Model Architecture

Our policy takes the prompt video and the current robot state as inputs and outputs robot actions. It consists of four modules: (1) prompt video encoder, (2) robot state encoder, (3) state-prompt encoder, and (4) robot action decoder. The entire architecture is illustrated in Figure 3, and each of the modules is detailed below:

(1) *Prompt Video Encoder* encodes the video demonstration provided as a reference to convey the desired task semantics. The prompt video encoder implicitly learns to infer what task to perform and how to do it. The prompt encoder consists of a per-frame Image encoder  $\phi_p$  (ViT [15]) followed by a Perceiver Resampler [1, 20]  $\psi_p$ . The output of the prompt encoder  $\psi_p(\phi_p(V)) = z_{prompt}$  is a set of  $N$  tokens of  $d$ -dimension to condition the policy with the task-relevant attributes from the video.

(2) *Robot State Encoder* encodes the current state of the robot given the current frame and last  $k$  frames as input. Note that this module also encodes information about the objects and environment visible to the robot. The architecture is similar to the prompt encoder: a per-frame Image encoder

$\phi_s$  followed by a Perceiver Resampler  $\psi_s$ . Identical to the prompt encoder’s outputs, the output of the state encoder is  $\psi_s(\phi_s(S_t)) = z_{state}$  that encodes the latent environment and robot state information from the history of recent observations. We use the same image encoder weights for both (1) and (2), that is,  $\phi_p = \phi_s = \phi$ . The role of the image encoder  $\phi$  is to capture spatial visual information in each frame. The perceiver resampler enables temporal learning across frames and reduces the number of video tokens passed into the action decoder.

(3) *State-Prompt Encoder* takes the prompt video encoding  $z_{prompt}$  and robot state encoding  $z_{state}$  and outputs a task encoding relevant for action prediction, which we call prompt-aware state tokens  $z_{state|prompt}$ . Here, the state encoding acts as queries, and the prompt video encoding acts as keys and values. Intuitively, the state-prompt encoder enables the fusion of the state and prompt information. Suppose a prompt video shows picking up an apple in the basket, and the current state contains an apple, a banana, and an orange. The State-Prompt Encoder cross-attends and learns which object to attend to in the state based on the prompt video. Capturing interdependencies between prompt and state is crucial for the next step of action decoding.

(4) *Robot Action Decoder* predicts the action vector  $a_t$  for the current state  $S_t$  such that it completes the task shown in the prompt video  $V_p$ . The action decoder is a transformer decoder architecture that uses the fixed action position tokens [53] as input queries and the prompt-aware state tokens  $z_{state|prompt}$  for keys and values. The size of the action position embedding is  $N \times d$  where  $N$  is the number of action dimensions, and  $d$  is the transformer embedding dimension. More details on action vector in §II-D.

The action position embeddings cross-attend to the prompt-aware state tokens to predict the target binned action values as output. Each output token of the action decoder corresponds to an action dimension for the mode, arm, and base. We project each token embedding to 256 dimensions, and a softmax layer is applied on the top to obtain the bin corresponding

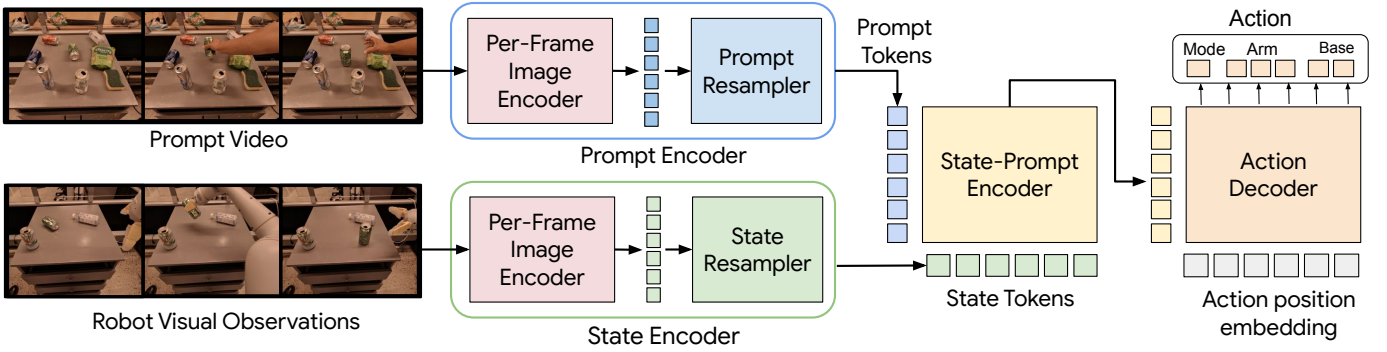


**Fig. 3: Architecture.** Our model takes the prompt video and the robot’s current observations as the input, encodes those into token embeddings for the prompt video and the robot’s state, cross-attends to produce state-prompt encoding, and translates it into the expected robot action at the current timestep. More details in Section II-C).

to the target action vector. Unlike prior work [8, 9] that use autoregressive action decoding that requires multiple forward passes during inference, we use action position embeddings for one forward pass prediction like in ACT [53]. Instead of predicting one action for the next timestep, we follow the approach outlined in [22, 53] and train the policy with a prediction horizon of four steps. We always use the action bin with the highest probability, that is,  $\text{argmax}$  over predicted probabilities, to choose the action value for execution.

*Cross-Attention Layers.* In the Vid2Robot architecture, we use Cross-Attention Transformer layers extensively in the following modules: Prompt Resampler, State Resampler, State-Prompt Encoder, and Action Decoder. Compared to standard self-attention layers, which require more memory to process the same video, cross-attention layers help manage the high number of tokens and the resulting large attention matrices when processing prompt and robot state videos. For example, when using ViT-B/16, the total number of video tokens for a 16 frame reference video and a 8 frame robot state video at  $224 \times 224$  resolution would be  $8 \times 196 + 16 \times 196 = 4704$ . An entire self-attention operation would lead to an attention matrix with  $4704^2 \sim 22\text{M}$  entries. However, using two Perceiver Resamplers with 64 latent tokens, we train with attention matrices of the size  $8 \times 196 \times 64 + 16 \times 196 \times 64 \sim .3\text{M}$ . Thus, cross-attention layers in Vid2Robot reduce attention computation and enable training with paired videos.

#### D. Preprocessing

To efficiently train videos of varying lengths, we randomly sample  $N=16$  frames. We always include the first and last frames and sort them in increasing order of time. We sample a robot state  $S_t$  during training by sampling a random timestep. We then select the preceding  $k-1$  frames to create a robot state video comprising a total of  $k=8$  frames before. If there are less than  $k-1$  frames before the current time step, we repeat the first frame to create a fixed-size robot state video. We normalize the pixel values in each frame between 0 and 1 and resize each frame to  $(224, 224)$ . During training,

we apply photometric distortions like cropping, brightness, contrast, hue, and saturation.

The action at that time consists of the three components: *Mode*: ( $m$ ) whether to terminate episode, move only arm, move only base, or both. *arm*: gripper position ( $x, y, z$ ), orientation (rotation along  $xy, yz, zx$ ), and the degree of closedness ( $c$ ). *Base*: displacement ( $x, y$ ) and rotation. Overall, the action  $a_t = [m, g_x, g_y, g_z, \theta_{xy}, \theta_{yz}, \theta_{zx}, c, b_x, b_y, b_\theta]$  is an 11-dimensional vector. Each value has different ranges, which we first use to scale the values between 0 and 1. We further discretize the values into 256 bins each. In this study, we train and evaluate scenarios where the base remains stationary.

#### E. Training

(1) *Action Prediction Loss.* We train Vid2Robot end-to-end with behavior cloning. We use a classification loss on actions discretized into  $N=256$  bins. Given the robot trajectory for performing a task with current visual observations  $x_t$ , we have the corresponding expert action  $a_t$ . The action prediction loss is Cross Entropy between the predicted action and the expert action as:  $L_{CE}(a_t, \hat{a}_t) = \sum_{\tau} a_t \log \hat{a}_t$ . This loss trains all the model parameters, as shown in Fig 3.

Although our dataset size is substantial, it is insufficient for training large transformer-based models. To prevent overfitting on the training set, we add three **auxiliary losses** to encourage learning features in prompt videos.

(2) *Video Alignment Loss:* We want to encourage temporal alignment between prompt videos and robot videos performing that show the same task. By aligning prompt videos with the robot videos, we want the image encoder to learn to be invariant to different embodiments, lighting, backgrounds, view angles, and distractor objects while still encoding features relevant to predicting task progress.

Our choice of loss is the temporal-cycle consistency loss introduced in [18]. This loss can encode the task progress when trained on videos of different agents performing the same task [51]. This loss is applied on per-frame image embeddings of the prompt  $V_p$  and robot  $V_r$  videos during training. To apply the loss, we average pool the per-frame

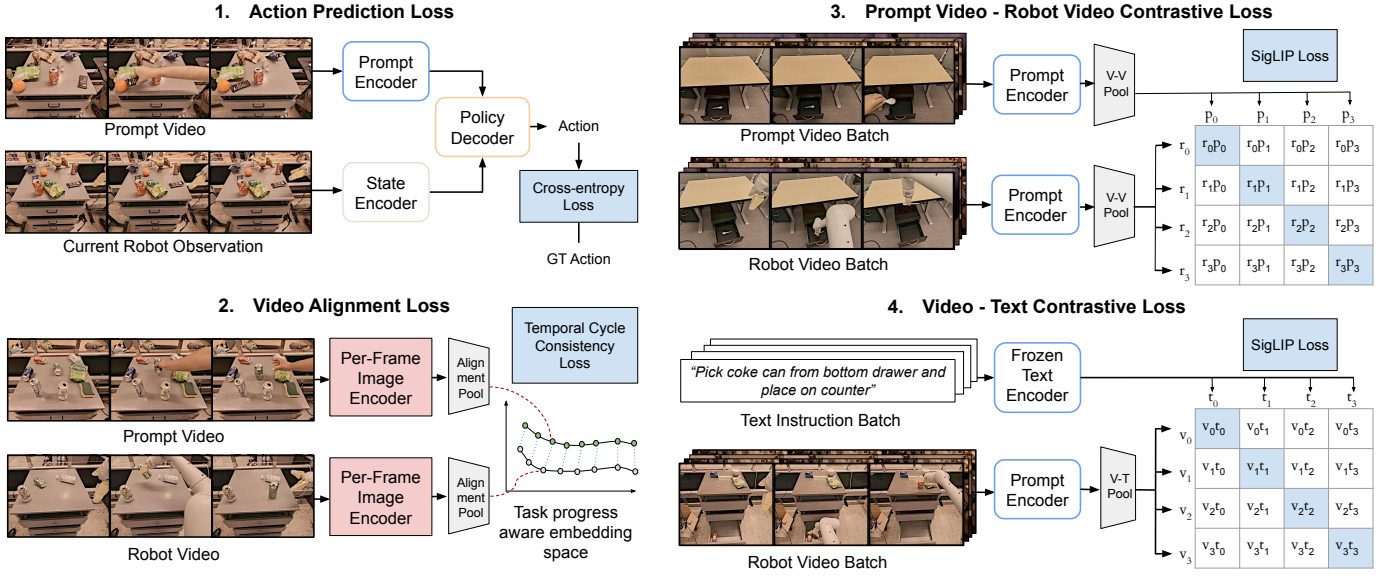


**Fig. 4: Training Setup.** We show all the losses used for training Vid2Robot, particularly how each loss connects to its different modules. Along with (1) the main action prediction loss, we apply three auxiliary losses: (2) temporal video alignment loss, (3) a contrastive loss between the prompt and robot video performing the same task, and (4) a contrastive loss between a prompt/robot video with the language embedding. More details are in Section II-E.

embeddings output in spatial dimensions from image encoder  $\phi$  and apply a projector head of 2-layer MLP [11]. We call this as *alignment pooling layer*  $\Phi$  on the per-frame image embeddings, as shown in Fig 4. For each video  $V_i$ , this results in a sequence of embeddings  $E_i = \{\Phi(v_i^1), \Phi(v_i^2), \dots, \Phi(v_i^{L_i})\}$ , where  $L_i$  is the number of frames in the  $i^{th}$  video. We apply TCC loss on encoding  $E_p$  and  $E_r$  for prompt and robot video, respectively. Intuitively, the TCC loss ensures that the representation of every frame of  $E_p$  should correspond to  $E_r$  and vice versa. Applying TCC in Vid2Robot involves two steps: First, we compute soft neighbor of  $t^{th}$  frame of  $E_p$  ( $E_p^t$  in short) in  $E_r$  and call it  $\widehat{E}_{pr}^t$ .

$$\widehat{E}_{pr}^t = \sum_k \alpha_k E_r^k, \quad \text{where} \quad \alpha_k = \frac{e^{-\|E_p^t - E_r^k\|^2}}{\sum_k e^{-\|E_p^t - E_r^k\|^2}} \quad (1)$$

Second, we find the corresponding frame for this newly computed soft-neighbor in  $E_p$ . This is called *cycle-back* in [18] and it involves similar soft-neighbour computation as in Equation 1 to obtain say  $\widehat{E}_{pr}^t$ , which ideally should be same as  $t$ , that is,  $(\widehat{E}_{pr}^t - t)^2$  should be minimized. TCC loss minimizes such mean squared error between all frames for prompt and robot video encodings, and vice-versa, that is,

$$L_{TCC}(E_p, E_r) = \sum_{t \in V_p} (\widehat{E}_{pr}^t - t)^2 \quad (2)$$

$$L_{TCC} = \frac{L_{TCC}(E_p, E_r) + L_{TCC}(E_r, E_p)}{2}$$

(3) *Prompt-Robot Video Contrastive Loss (VVCL)*: We want to encourage the prompt encodings to learn task semantics from video tokens in a self-supervised manner. While we pair prompt and robot video using natural language, this does not

effectively capture the visual similarity of low-level motions like reaching for objects and rotating the robot arm. For this, we apply contrastive loss between the latent features of the robot and the prompt videos. We use an Attention Pooling layer to merge features from the  $N$  prompt tokens to produce a single embedding for each video. We apply the SigLIP [52] loss between video-video pairs to encourage videos showing the same task, involving similar motions and interacting objects, to be close to each other while being away from other videos in the batch. A batch contains the same number of robot and prompt videos, say  $B$ . We use the prompt encoder  $\psi_p(\phi(\cdot))$  to obtain a batch of full robot video embeddings  $Z_{robot}$  and prompt video embeddings  $Z_{prompt}$ , each of size  $B \times d$ . We multiply them,  $Z_{robot} \cdot Z_{prompt}^T$  to obtain a  $B \times B$  matrix. Adding a learnable temperature  $\tau$  and bias  $b$ , we have our logit matrix as  $\hat{Y} = (Z_{robot} \cdot Z_{prompt}^T) * \tau + b$ . We consider the videos of robot and prompt performing the same task as positives and assign them a label of 1 along the diagonal and -1 for off-diagonal pairs, that is, the label matrix  $Y = 2I_B - 1$ . SigLIP loss is the negative loglikelihood  $\sigma'(Z_1, Z_2) = -\sum \log \sigma(Y \cdot (Z_1 \cdot Z_2^T) * t + b)$ . The video-video contrastive loss is as follows:

$$L_{VVCL} = \sigma'(Z_{prompt}, Z_{robot}) \quad (3)$$

(4) *Video-text Contrastive Loss (VTCL)*: We want to encourage a part of the embedding space to be aware of object names and verbs, as shown in the prompt and the robot videos. We apply a contrastive loss between prompt tokens produced by the robot video and the text instructions of the task. A version of this loss has been applied before by BC-Z [22] as auxiliary language regression loss. We use an Attention Pooling layer [50] with one latent query to merge features

from the  $N$  prompt tokens to produce a single embedding for each video. We retrieve  $B$  pairs of video and text embeddings as a batch. Similar to Equation 3, we apply SigLIP [52] loss as  $L_{VTCL}$  to encourage every video to have similar embeddings to their textual description embeddings, and be different from other text embeddings in the batch.

$$L_{VTCL} = (\sigma'(Z_{prompt}, Z_{text}) + \sigma'(Z_{robot}, Z_{text}))/2 \quad (4)$$

Overall, we apply the mean of all four losses for training that is  $L = \frac{1}{4}(L_{CE} + L_{TCC} + L_{VVCL} + L_{VTCL})$ .

### F. Implementation

We trained the model (implemented in Jax) for 200K iterations. We use AdamW optimizer with an initial learning rate of  $8e-5$  using a cosine learning rate schedule with warmup steps 2,000 and a final learning rate of  $1e-6$ . We use 2 Perceiver Resampler layers with 64 latent tokens for both the Prompt and State Resamplers. Both state-prompt encoder and action decoder are 4-layer deep cross-attention transformers.

## III. EXPERIMENTS

We present results with real robot evaluations for our multi-task video-conditioned policy. One of the fundamental questions we tackle in this work is how well robots can imitate humans performing manipulation tasks. Because of differences in embodiments, humans perform manipulation tasks at a different speed and style. We study the effect of using robots and human videos as prompts.

**Metrics.** A *rollout* as a sequence of actions inferred from the policy and executed on the robot from an initial state observation until the policy terminates or takes the maximum number of steps, whichever is lower.

We define *success* for a rollout when the policy executes the task instruction as shown in the prompt video. A successful rollout involves correct actions to be taken successively in the environment without any assistance for resets or recovery. We ask a human evaluator to observe whether: (1) whether the robot *reached* the correct location?, (2) *grasped* the correct object?, (3) *released* the object at the correct location?, and (4) *terminated* the task correctly?

If the answer to any question is “no”, the answer to subsequent questions is assumed to be “no”. If all questions are answered “yes”, only then the rollout is considered “successful”. For each task instruction, we record a few rollouts per policy with different distractor objects, background, and lighting conditions. We take the average success recorded across all the rollouts for a task and call it that task’s *Success Rate*. We also report aggregated success rate across tasks as *Overall Success Rate*. We also analyze the partial success across the four milestones in Section III-A.

We looked into automating success detection with concrete criteria or decision rules for evaluation but found that this automation can overlook the *process* of performing the task. Consider the task of “knocking the water bottle over”. *Case 1*: The robot successfully grasps the bottle, turns it, and places it on the table. *Case 2*: The robot fails to grasp, pinches the bottle

away, and lands in a knocked-down orientation. While Case 1 is desired and expected behavior according to the training data, Case 2 is a failure as it is unintended. With rule-based verification of the final state, we would have deemed both Case 1 and 2 successful. With human evaluators, we focus on the entire process of achieving the task instead of the final state.

**Setup.** We evaluate the policies by varying the object placement, lighting conditions, background surfaces, and distractor objects. When evaluating a set of policies, we ensure comparable initial object configurations for rollouts. We randomize the initial state only after all policies’ rollouts have been performed. For all rollouts, we sample prompt videos not seen during training. In all the experiments, we use a mobile manipulator, the Google Robot. It has an ego-centric camera view, a single arm with seven degrees of freedom, and a two-fingered soft gripper. Refer to [8] for more details.

**Baselines.** We compare our model with BC-Z [22], a video-conditioned policy using a ResNet-18 encoder. BC-Z [23] processes demonstration-observation pairs via a FiLM [38] conditioned ResNet encoder and feeds into a ResNet-based policy network to predict robot actions. We use the same data to train the BC-Z and Vid2Robot for a fair comparison. BC-Z does not have a terminate action, so we run these rollouts for a fixed maximum number of steps.

**Key Questions and Results.** We address the following questions in this work: (1) What is the success rate gap due to prompt embodiment (robot vs. human) across tasks? (§III-A1) (2) How do video-conditioned policies perform with unseen task videos? (Fig 5, §III-A2) (3) Is Vid2Robot’s overall success significantly better than BC-Z baseline? (§III-B) (4) Can learned motion representations handle out-of-distribution object interactions? (§III-C)

### A. Task-based success

We compare our Vid2Robot model and baseline BC-Z with robot- and human-performed prompt videos in Table I. We train both Vid2Robot and BC-Z on the same data mixture containing robot-robot and human-robot paired data. Prompt videos cover a subset of the training tasks. However, the videos are unseen by the models. In this evaluation, we investigate each model’s ability to infer the task specification from the prompt video as well as the current observed state of the robot.

To test the model’s capabilities in different settings on real robots, we assess rollouts on the following nine tasks: ‘knock water bottle over’, ‘move rxbar chocolate near coke can’, ‘move green jalapeno chip bag near coke can’, ‘pick green rice chip bag’, ‘place coke can upright’, ‘pick coke can from bottom drawer and place on counter’, ‘open middle drawer’, ‘close middle drawer’, and ‘place apple into top drawer’.

We ask four evaluators to carry out two rollouts per task for a prompt video dataset and policy setting (a row in Table I). Overall, we have eight trials per task to evaluate a policy’s task success rate. We report an overall success rate per row over nine tasks with eight trials per task, that is,  $9 \times 8 = 72$  trials. In total, we required  $72 \times 4 = 288$  rollouts for Table I.

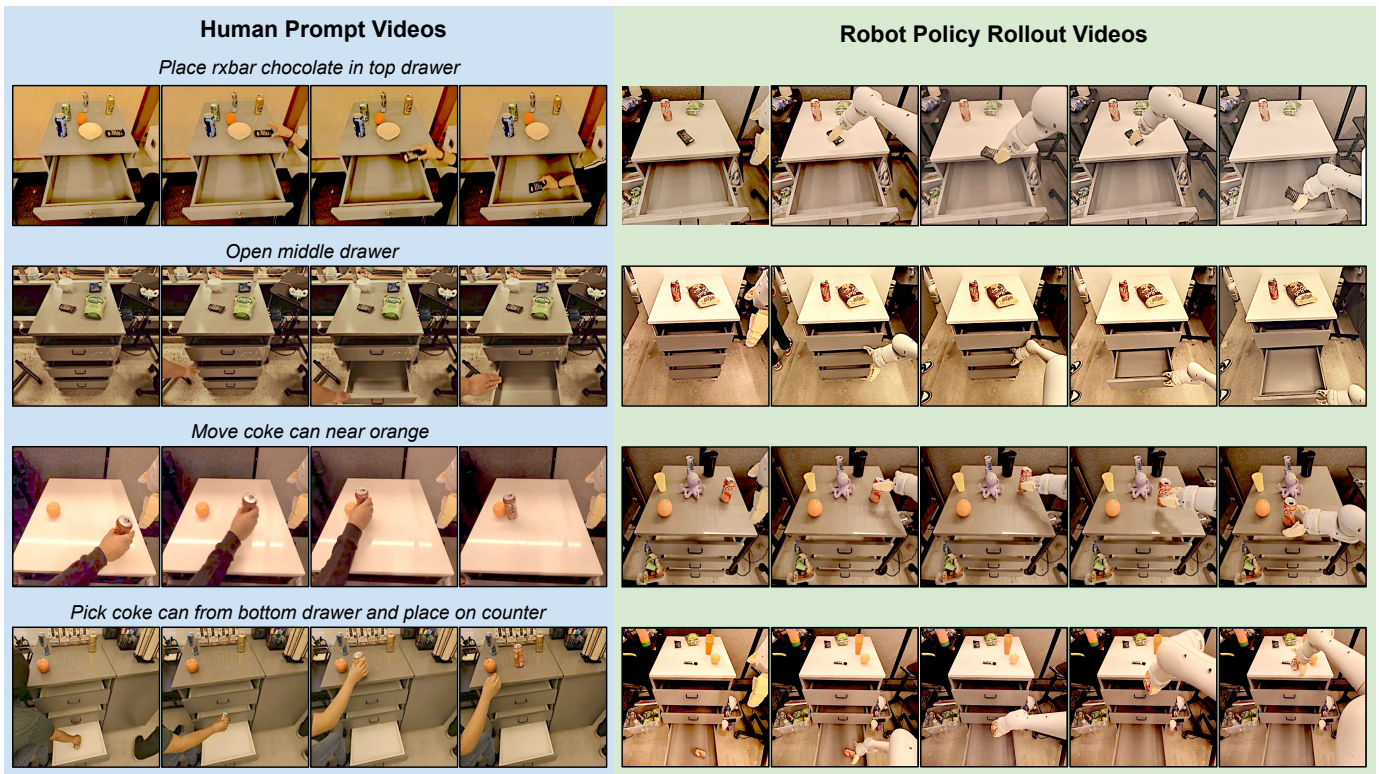


**Fig. 5: Policy Rollouts.** Each row shows a prompt video of a human doing a task on the left, and on the right, we show the corresponding successful robot rollouts using Vid2Robot. Note how visually different the prompts are, while the policy rollouts have different lighting and backgrounds, as well as the number and placement of the distractor objects.

**TABLE I: Task Success Rate for Robot and Human prompts.**

| Prompter | Model     | <i>pick</i>   | <i>pick-place on</i> | <i>place into</i> | <i>open</i>  | <i>close</i>  | <i>move near</i> | <i>knock over</i> | <i>place upright</i> | Overall      |
|----------|-----------|---------------|----------------------|-------------------|--------------|---------------|------------------|-------------------|----------------------|--------------|
| Robot    | BC-Z      | 75.0%         | 50.0%                | <b>61.5%</b>      | 16.7%        | 66.7%         | <b>44.0%</b>     | <b>58.3%</b>      | <b>50.0%</b>         | 52.6%        |
|          | Vid2Robot | 75.0%         | <b>58.8%</b>         | 50.0%             | <b>91.7%</b> | <b>100.0%</b> | 33.3%            | 41.7%             | 16.7%                | <b>54.9%</b> |
| Human    | BC-Z      | 50.0%         | 12.5%                | 12.5%             | 0.0%         | 50.0%         | 43.8%            | 12.5%             | <b>50.0%</b>         | 30.6%        |
|          | Vid2Robot | <b>100.0%</b> | <b>50.0%</b>         | <b>50.0%</b>      | <b>62.5%</b> | <b>87.5%</b>  | <b>43.8%</b>     | <b>25.0%</b>      | 12.5%                | <b>52.8%</b> |

1) *What is the gap in success rate due to embodiment difference in prompt videos?:* When prompted with robot and human videos, we compare our model with BC-Z, which is a strong baseline for our comparisons. The overall success rate of our model Vid2Robot outperforms BC-Z for Human prompt videos by 20%, and is comparable for Robot prompt videos. Note that there is an order of magnitude more training samples for robot trajectories than human videos in our training mixture. Hence, there isn't a significant gap in performance for robot prompt videos. Our model outperforms BC-Z in most tasks for human prompt video, showing that Vid2Robot captures the task semantics from prompt videos better than the baseline. Our model outperforms in tasks like picking something from a drawer, placing it on the counter, and opening/closing drawers by a large margin. The most challenging task is *placing upright* and *knocking over*. We analyze the failure reasons in §V Fig 9.

2) *How well do video-conditioned policies perform when shown a task in an unseen video?:* In addition to marking a

rollout as a success, we recorded partial success annotations per rollout. In Fig 6, we observe that our model *reaches* to the correct object 78%, about 8% more than baseline. The policies sometimes fail to get the correct object and go towards a distractor instead. Next, *grasping* errors happen, particularly with small and deformable objects and collision-prone areas like drawer handles or counter's edges. Here, our model (65%) outperforms BC-Z (45%) by a large margin of 20% — a successful grasp is often the most challenging part of a rollout and crucial for success. After grasping, most tasks require *releasing* at a correct location. Both models slightly drop in success rate due to incorrect *release* during the rollouts. While BC-Z runs for a fixed number of steps, our policy Vid2Robot predicts when to terminate. We observe that the rate of *release* and *terminate* is almost identical, about 57% for our model, which implies that after releasing at the correct location, Vid2Robot mostly terminates successfully.

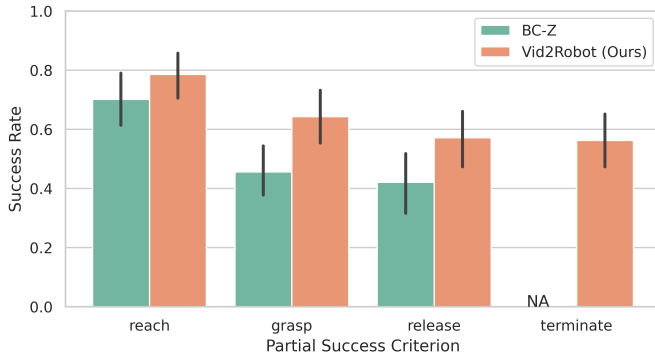


**Fig. 6: Partial Success Rate for BC-Z and Vid2Robot.** Our policy Vid2Robot outperforms BC-Z in terms of *reaching* the correct object, *grasping* it, *releasing* it at the correct location and then *terminating* the episode correctly. Note that BC-Z does not have terminate control.

**TABLE II: Real Robot Evaluation of Vid2Robot and BC-Z with more trials to ascertain the statistical significance of the results.**

| Model     | place coke can upright | close middle drawer | Overall            |
|-----------|------------------------|---------------------|--------------------|
| BC-Z      | 19.4 ± 9.5%            | 39.2 ± 10.8%        | 30.2 ± 7.1%        |
| Vid2Robot | <b>39.1 ± 9.9%</b>     | <b>48.7 ± 11.2%</b> | <b>43.4 ± 7.2%</b> |

### B. Tasks with More Rollouts

To comment on the statistical significance of our results, we conducted more trials while limiting the evaluation to two tasks, namely ‘place coke can upright’ and ‘close middle drawer’ for real robot policy evaluations, and reported mean success rate with confidence intervals. In total, we conducted 314 real robot rollouts for results reported in Table II.

### C. Cross-object motion transfer

We trained our Vid2Robot and baseline with paired videos as discussed in Section II-B. Due to the pairing, the training data included only those scenarios where the interaction object shown in the prompt is present in the current robot observations. But *what if we provided a prompt video of one object and tested on other objects? Does it make the same motion as shown in the prompt video?* Interestingly, we found our model to perform learned manipulation actions on objects not seen in the prompt video. We call this emergent behavior as *cross-object motion transfer*.

We compare Vid2Robot with BC-Z for cross-object motion transfer ability with five prompt videos, namely, ‘knock water bottle over’, ‘pick green rice chip bag’, ‘place coke can upright’, ‘pick coke can from bottom drawer and place on counter’, and ‘place apple into top drawer’. We evaluate each case of a prompt video by placing unrelated objects in robot’s initial observation. The objects used for evaluation are ‘orange’, ‘green can’, ‘chips bag’, ‘banana’, ‘pink piggy soft toy’, ‘wrist watch’. We selected objects with different shapes, sizes, and deformability to evaluate situations requiring different grasps for success.

The evaluation setup is similar to Section III-A. Here, the evaluator sets up one of the objects for a task and records

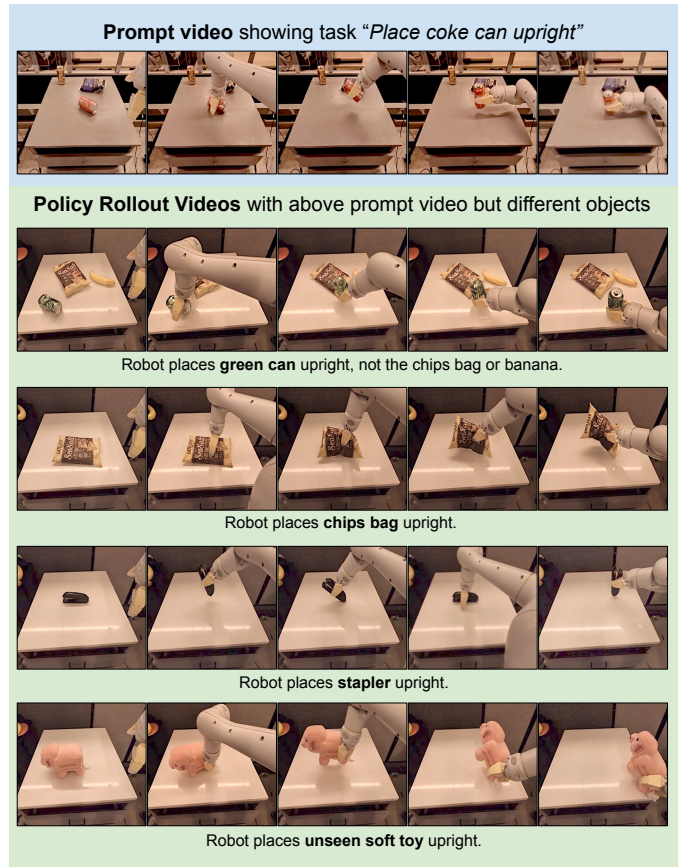


**Fig. 7: Qualitative results for cross-object motion transfer.** (Top-blue) Prompt video of *placing coke can upright*; (Green) Policy rollouts with a *green can*, *chips bag*, *stapler* and a *soft toy* in front of the robot. Vid2Robot infers the motion of *place upright* in the prompt video and applies it to other objects. The policy adheres to the prompt video by picking the green can instead of the chips bag or banana.

rollouts for each model. We compare two models on five tasks with six objects, so every evaluator runs  $2 \times 5 \times 6 = 60$  rollouts. We repeat the evaluation with four raters, thus reporting results in Table III on  $4 \times 60 = 240$  rollouts.

In Fig 7, we show the above experimental setup qualitatively. We use a prompt video to ‘place coke can upright’ and observe that the policy can transfer the action of ‘placing upright’ to objects, like a green can, a chips bag, a stapler, and a soft toy. The policy shows an implicit notion of learned pragmatics, by selecting green can over other objects.

In Table III, we observe that BC-Z is often unable to complete the tasks when testing cross-object motion transfer. In contrast, our model (34%) performs better than BC-Z (17%) in this setting and performs the motion indicated in the prompt video. Our model is comparable to BC-Z with a 45% success rate on *picking* out-of-distribution objects. More importantly, tasks involving placing into drawers demonstrate significant improvement (29% → 54%). For specific tasks like *picking from drawers*, *placing on counters*, and *knocking over*, Vid2Robot completes the task 25%–29% of the time, whereas BC-Z is unable to perform.



TABLE III: Cross-object motion transfer success.

| Model     | <i>pick</i> | <i>pick-<br/>place on</i> | <i>place<br/>into</i> | <i>place<br/>upright</i> | <i>knock<br/>over</i> | Overall      |
|-----------|-------------|---------------------------|-----------------------|--------------------------|-----------------------|--------------|
| BC-Z      | 45.8%       | 0.0%                      | 29.2%                 | 12.5%                    | 0.0%                  | 17.5%        |
| Vid2Robot | 45.8%       | <b>25.0%</b>              | <b>54.2%</b>          | <b>16.7%</b>             | <b>29.2%</b>          | <b>34.2%</b> |

#### D. Ablations

We analyze our proposed approach to understand the following: (a) Can the policy learn possible interactions with the environment from state observations alone, without needing prompt videos? (b) How do the auxiliary loss functions impact the model’s performance?

1) *What is the impact of the prompt for task inference?:* First, we motivate the importance of prompt videos with an example. Consider a Coke can and other objects on the countertop as the robot’s state observation. If a Coke can exists in the robot’s view, it is hard to infer whether the task is to “pick a Coke can”, “move a Coke can close to a chocolate bar”, “move a Coke can near an orange can,” or “knock over Coke can”. Furthermore, once the robot starts taking action, it can end up in new states, like being close to rxbar, which make it especially difficult to predict tasks from the current state only. Below, we empirically measure the success rate of a policy that does not have access to a suitable prompt video.

We evaluated the “no-prompt” case, in which both models see blank frames as input prompt videos. In this setup, we evaluated three tasks. For each task, we rolled out the policy 20 times. In total, we ran  $2 \times 20 \times 3 = 120$  actual robot rollouts for this experiment. Here, the success rate is 23% for Vid2Robot and 5% for BC-Z over 20 rollouts per task per policy. We find that performance improves when we condition the policies on the prompt videos. The success rate improves from 5% to 52.6% for BC-Z and from 23% to 54.6% for Vid2Robot. (Refer Table I). This experiment underlines the importance of prompt videos for task success.

2) *What is the role of auxilliary losses?:* Second, we analyze the role of additional loss functions in the overall success rate. In Section II-E, we presented action prediction loss and three auxiliary losses. We investigate the impact of (1) not using any auxiliary loss and (2) adding auxiliary language loss. We consider the tasks similar to those described in Section III-A, 9 tasks for evaluating each policy. We have 3 model variants: the original Vid2Robot, the one without video-text contrastive loss (CL), and the one with only action prediction loss. We ask three human evaluators to run a model variant for two rollouts each. In total, we report results with  $3 \times 3 \times 9 \times 2 = 162$  rollouts in Fig 8. The error bars show the standard deviation for success.

*What is the impact of not using any auxiliary loss?* We observe that the performance of our model (61%) improves significantly by enforcing representation constraints through auxiliary losses, compared to using only action prediction loss (45%). It highlights the importance of the proposed auxiliary losses in Section II-E.

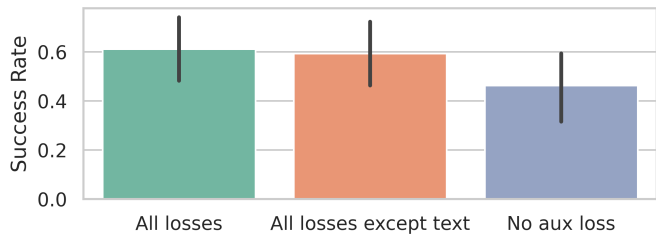


Fig. 8: Ablation for auxilliary losses used in Vid2Robot. We compare our proposed approach that has all auxiliary losses (green, left) with a variant without language contrastive loss that was originally proposed in BC-Z (orange, middle) and a version with no auxilliary losses (blue, right). More details in (§III-D)

*What is the impact of the auxiliary language loss?* BC-Z proposed to use language representations to improve video representations for conditioning the policy. We compare our policy with another variant trained with all losses but the Video-Text CL. We observe only a borderline improvement of 1-2% in the success rate when using language loss. This implies that video alignment and video contrastive loss contribute significantly towards performance improvement.

## IV. RELATED WORK

### A. Task Specifications for Robots

The development of general-purpose robots hinges on effectively grounding task specifications. Videos are a dense source of information that provides information about what to do and how to do it in the physical world. Recent works have used videos for task specification [4, 24, 42]. Another line of work uses videos to learn world models to predict future visual observations [31, 28, 10, 33, 16].

Recall our example of “open drawer”, “open cabinet”, and “open jar” in the §I. Video-conditioned policies like Vid2Robot are capable of doing these tasks because these policies identify the tasks of “open jar” and “open drawer” from visuals, unlike language-conditioned which have the same embedding of the verb ‘open’ for each task. Note that language is not an input to Vid2Robot. Therefore, the verb does not directly influence the action; this is a critical difference between Vid2Robot and existing language-conditioned robot policies. While language [49, 8, 35, 36], final goal images [25, 7], and others like hand-drawn inputs [45] have been proposed as means for task specification, learning from prompt videos is complementary to these approaches and inevitable for rapid adaptation of trained polices to perform new manipulation skills at deployment.

### B. Learning from Human Demonstrations

As videos of humans performing various tasks proliferate on the internet, several works aim to address how to leverage this information for robot learning. The difference in robot versus human embodiment poses a significant challenge, for which existing approaches range from translating the image of a human into the robot [44] to inpainting for agent-agnostic

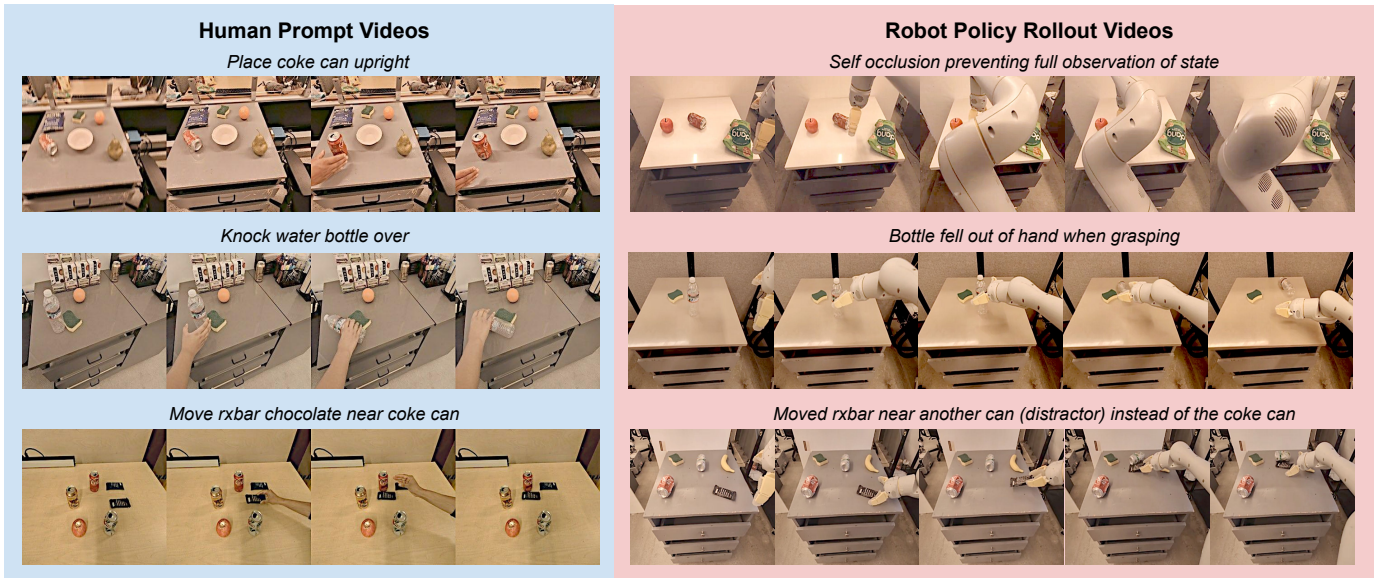


**Fig. 9: Failure analysis with policy rollouts.** (Top) Policy predicts gripper pose and depends on the IK solver to move the arm. Sometimes, the IK solution can block the robot’s camera view. (Middle) Grasping failures happen, especially with transparent and deformable objects. (Bottom) Distractor objects and differences in lighting and background may cause recognition errors, where policy might perform the correct motion but with an incorrect object(s).

representations [3]. Many prior works propose to leverage off-the-shelf models for hand pose estimation and contact tracking [5, 13, 39], object-centric representations [40, 21], as well as reward functions for reinforcement learning [3, 29, 44].

XIRL [51], GraphIRL[26] and other RL approaches [41, 37] take a lot of time and manual effort for resetting scenes during the policy learning phase, limiting their applicability to real robots. Furthermore, RL often leads to unsafe situations with real-world robots. We compare Vid2Robot to another end-to-end behavior cloning method, BC-Z, that has been shown to scale to multiple tasks. Other methods [34, 47, 5] cast this problem into visual representation learning to accelerate learning of downstream motor control tasks. While these modular learning solutions work well in limited datasets, they are prone to compounding errors in each component and are not efficiently scalable. End-to-end training approaches for goal-conditioned imitation learning [12, 43, 19, 14] are also largely limited in simulation and hindered by sim-to-real gap. In contrast, we tackle this as an end-to-end large multi-task learning from human videos with real robot evaluations.

### C. Imitation via Paired Demonstrations

Our setup of paired prompt videos and robot trajectory is most similar to the One-Shot Visual Imitation literature. Many prior works assume access to pairs, where the first video demonstrates the task, and the second video shows the agent’s visual observations. Some of the early works [17] proposed training a demonstration network via temporal convolution and neighborhood attention to condition a manipulation policy network. In more recent approaches like [12, 30, 21], paired demonstrations and observations are used to train a transformer policy, often with additional constraints like inverse dynam-

ics prediction[12] or contrastive representation learning [30]. MimicPlay [46] proposes hierarchical learning framework using human and robot teleoperated demos. However, evaluating these approaches is usually limited to a specific set of tasks, without any changes in background between the two videos.

BC-Z [22] is most similar to our work, which reports real robot evaluations. While our training setup has similarities with BC-Z, our model Vid2Robot couples large image encoders, cross-attention layers, and contrastive auxiliary losses to learn a manipulation policy that imitates a human showing a task. Recent approaches for self-supervised skill discovery like XSkill [48] learn skills from unpaired human and robot videos, while our approach uses text descriptions of the task to pair them explicitly. The paired human and robot videos contain different backgrounds, lighting, and object arrangements, thereby training the visual representations to be invariant to these settings, and focus on the task semantics instead.

## V. LIMITATIONS AND FUTURE DIRECTIONS

In Sec III, we show that our approach has improved over previous work but there is a gap in performance for video-conditioned policies. Below we discuss the limitations of our work and provide insights for the future.

First, we qualitatively investigate some reasons for the failure of a policy rollout. In Fig 9, we illustrate and explain three examples of how self-occlusion, grasping errors, and the presence of distractors can lead to failure during any rollout.

Second, we observe a significant drop in the grasping success in Figure 6. While we use robot camera observation to estimate the state and implicitly learn depth estimation, it is often incomplete when occlusion or the robot gripper is out of

camera view. Enhancing the state information with multimodal sensor fusion may improve the grasp success rate.

Third, we consider carefully collected short task instruction demonstrations from three different sources as shown in Section II-B, all of which are 5 to 20-second videos. To test our models on long-horizon demonstrations or ‘in-the-wild’ videos online, we need effective pairing strategies for videos and a few corresponding robot trajectories to train the policy.

## VI. CONCLUSION

We present Vid2Robot, an end-to-end video-conditioned robot policy. Our proposed system trains on paired videos such that both videos demonstrate the same task but differ in diverse settings of lighting, background, and distractor objects. We use cross-attention (i) to learn the joint latent representations from prompt and state encodings and then (ii) to decode the action. We train the entire model for action prediction with cross-entropy loss and three auxiliary losses that encourage learning of generalizable latent representations to infer tasks directly from raw pixels to suitable actions. Vid2Robot outperforms BC-Z by over  $\sim 20\%$  when prompted with human videos. Further, Vid2Robot outperforms BC-Z by  $\sim 17\%$  for cross-object motion transfer; that is, if the prompt video didn’t have the exact object as the object the robot is manipulating now, the model still produces valid actions for the same verb but different objects. Cross-object motion transfer is a promising direction for further extending pragmatic transfer learning of motion to new objects. We hope Vid2Robot enables bootstrapping data collection and human-robot interaction with rapid adaptation to new skills.

## ACKNOWLEDGEMENTS

We would like to thank Yansong Pang, Grecia Salazar, Utsav Malla, Deeksha Manjunath, Jornell Quiambao, Sarah Nguyen, Sangeetha Ramesh, Tran Pham, Samuel Wan, Tomas Jackson, Jodilyn Peralta, Celeste Barajas, Elio Prado, Rochelle Dela Cruz, Alex Luong and Krista Reymann for supporting data collection via teleoperation. Special thanks to Jornell Quiambao, Grecia Salazar, Utsav Malla, Deeksha Manjunath, Sarah Nguyen, Sangeetha Ramesh, and Jaspiar Singh for evaluations on robot; Michael Ahn, Anthony Brohan and Keerthana Gopalakrishnan for policy evaluation infrastructure; Suneel Belkhale, Dorsa Sadigh, Chelsea Finn, and Sergey Levine for helpful discussions; Jonathan Tompson, and Vincent Vanhouke for thorough feedback on the writing. This work was performed by the first author as an intern at Google DeepMind Robotics. This work was also supported is partially funded by an unrestricted gift from Google and by the Defense Advanced Research Projects Agency (DARPA) under Agreement No. HR00112490375.

## APPENDIX

In our video provided in the supplementary materials, we show several examples of successful rollouts, and model architecture with prompt video and robot observations. We

provide specific examples of task-based success, and cross-object motion transfer. Additionally, we provide qualitative results on long-horizon task composition and rollouts for tasks that are rare in our training dataset. Finally, we provide rollouts of noted failures like case of self-occlusion, grasping errors and ambiguous interpretation of the task in the prompt video.

We will release the model code and trained checkpoints. In Table IV, we present the detailed version of the Vid2Robot model architecture. In Table V, we present the hyperparameters used while training. We also add data augmentations to the videos while training as per the settings in Table VI. We normalize the videos as required for the pre-trained ViT model.

We created the dataset mixture from the three sources. We collected 120k robot trajectories, 5k human trajectories, and 5k co-located human and robot trajectories. To create pairs, we sampled 3 videos as prompts per robot trajectory. This gives 360k pairs for Robot-Robot, about 15k pairs for Hindsight Human-Robot and 5k pairs for Co-located Human-Robot datasets. To ensure that all pairs are approximately sampled equally, we create the mixture proportions as 90% Robot-Robot, 5% Hindsight Human-Robot and 5% Co-located Human-Robot.

We also test Vid2Robot on some tasks which are rare in the training set and find that video-conditioned models are also able to complete them. Some examples of these tasks are: *opening glass jar*, *picking up green micro-fiber cloth* and *pulling out napkin*. We show examples in Fig. 10. For the video version of these results please take a look at the supplementary video.

In all the experiments in this paper, we use mobile manipulators. These robots have a 7 degree-of-freedom arm, a two-fingered gripper, and a mobile base. As the focus of our experiments is on manipulating objects, we keep the base fixed for each episode.

We test the policy with client-server setup, where the policy is deployed as server, which on-robot client can query. The observations from the head camera of the robot are recorded on the client side, to maintain a recent history of 8 frames. Based on the average response time from the policy, we can execute predicted actions at approximately 5-7 Hz.

We show Vid2Robot can perform long horizon tasks by using multiple prompt videos showing different tasks. To do so, we chain different prompt videos together to create a long horizon task. For example, Vid2Robot can be used to prompt a robot to *clean up the objects on a table into the drawer* by chaining prompt videos of 3 tasks: *open the drawer*, *place object on table into drawer*, and *close the drawer*.

When Vid2Robot outputs terminate episode for the current prompt video, we change the prompt video to be the next sub-task without resetting the robot. In this manner, the robot can complete long horizon tasks with Vid2Robot without explicitly being trained on long horizon videos. We show successful examples in Fig. 11. For videos of the robot completing long-horizon tasks, check the summary video in the supplementary material.

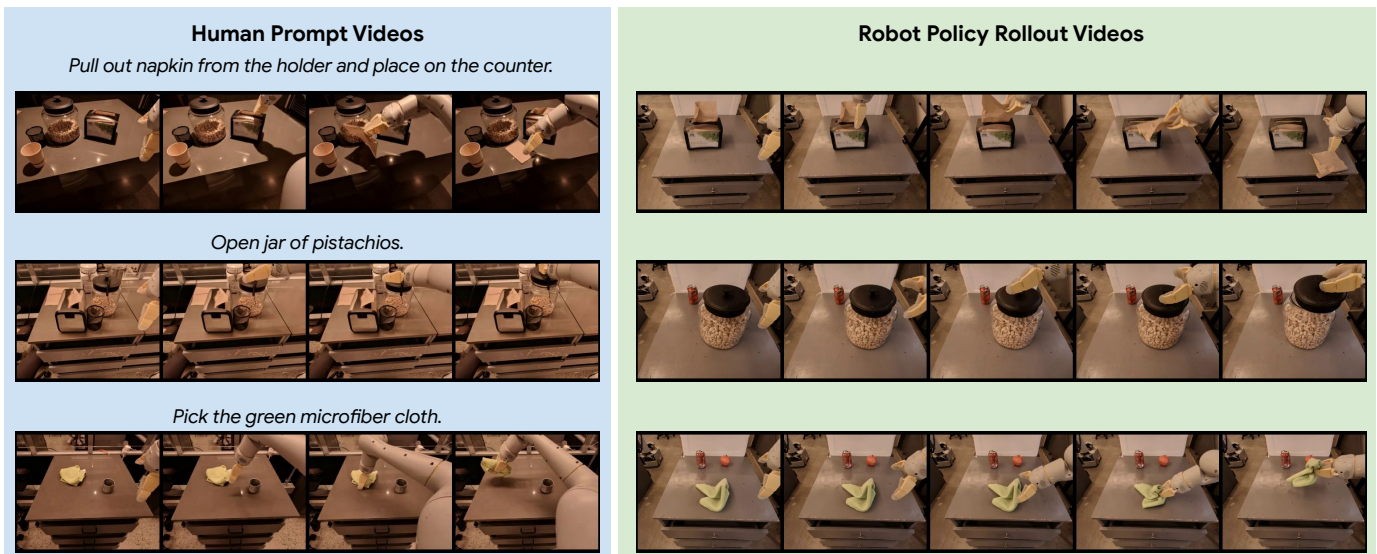


**Fig. 10:** Qualitative results on rare tasks.

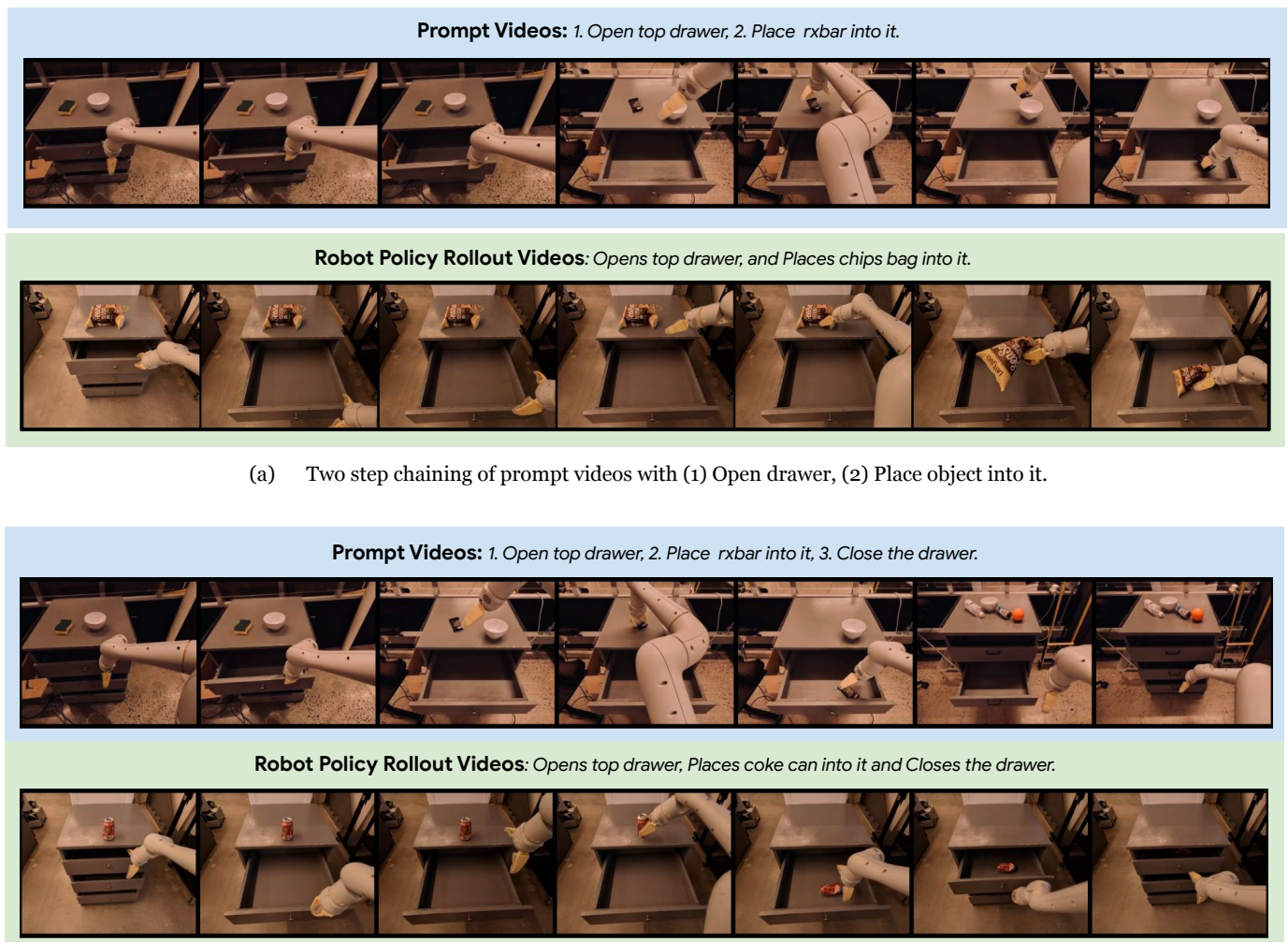


**Fig. 11:** Qualitative results showing how Vid2Robot can perform long horizon tasks with chaine prompt videos.

TABLE IV: Detailed Architecture of Vid2Robot.

| Module               | Layer                                | Output Size                         | Notes  |
|----------------------|--------------------------------------|-------------------------------------|--|
| Prompt Encoder       | Input                                | $16 \times 224 \times 224 \times 3$ | Reference Video of 16 frames   |
|                      | Image Encoder                        | $16 \times 196 \times 768$          | Each frame passes through ViT-B/16   |
|                      | Reshape                              | $3136 \times 768$                   | Reshapes all space-time tokens to be in one dimension  |
|                      | Perceiver Resampler                  | $64 \times 768$                     | 2 layers with 768 dims and 12 attention heads  |
| State Encoder        | Input                                | $8 \times 224 \times 224 \times 3$  | Robot Observation Video of 8 frames  |
|                      | Image Encoder                        | $8 \times 196 \times 768$           | Each frame passes through ViT-B/16   |
|                      | Reshape                              | $1568 \times 768$                   | Reshapes all space-time tokens to be in one dimension  |
|                      | Perceiver Resampler                  | $64 \times 768$                     | 2 layers with 768 dims and 12 attention heads  |
| State Prompt Encoder | Cross-attention<br>Transformer Layer | $64 \times 768$                     | 4 layers of cross-attention with 768 dim and 8 attention heads<br>Uses prompt tokens as keys and state tokens as queries                           |
|                      | Cross-attention<br>Transformer Layer | $11 \times 768$                     | 4 layers of cross-attention with 768 dim and 8 attention heads<br>Uses prompt-aware state tokens as keys and action position embeddings as queries |
| Action Decoder       | Cross-attention<br>Transformer Layer | $11 \times 768$                     | 4 layers of cross-attention with 768 dim and 8 attention heads<br>Uses prompt-aware state tokens as keys and action position embeddings as queries |
|                      | Linear                               | $11 \times 256$                     | Projection of action decoder output to 256 bins  |

TABLE V: Hyperparameters for Vid2Robot.

| Hyperparameters    | Values  |
|--------------------|---------|
| Batch size         | 2048    |
| Learning rate      | $8e-5$  |
| Optimizer          | AdamW   |
| Num training steps | 200,000 |
| Warmup steps       | 2000    |
| Image size         | 224     |
| Num prompt frames  | 16      |
| Num robot frames   | 8       |
| Prediction Horizon | 4       |

TABLE VI: Data augmentation for training Vid2Robot.

| Hyperparameters   | Ranges     |
|-------------------|------------|
| Height crop range | (0.95, 1.) |
| Width crop range  | (0.95, 1.) |
| Brightness range  | (0.9, 1.1) |
| Contrast range    | (0.8, 1.2) |
| Hue range         | (0, 0.03)  |
| Saturation range  | (0.8, 1.2) |

REFERENCES

[1] Jean-Baptiste Alayrac, Jeff Donahue, Pauline Luc, Antoine Miech, Iain Barr, Yana Hasson, Karel Lenc, Arthur Mensch, Katherine Millican, Malcolm Reynolds, Roman Ring, Eliza Rutherford, Serkan Cabi, Tengda Han, Zhitao Gong, Sina Samangooei, Marianne Monteiro, Jacob Menick, Sebastian Borgeaud, Andrew Brock, Aida Nematzadeh, Sahand Sharifzadeh, Mikolaj Binkowski, Ricardo Barreira, Oriol Vinyals, Andrew Zisserman, and

Karen Simonyan. Flamingo: a visual language model for few-shot learning. In Alice H. Oh, Alekh Agarwal, Danielle Belgrave, and Kyunghyun Cho, editors, *Advances in Neural Information Processing Systems*, 2022. URL <https://openreview.net/forum?id=EbMuimAbPbs>.

[2] Montserrat Gonzalez Arenas, Ted Xiao, Sumeet Singh, Vidhi Jain, Allen Z. Ren, Quan Vuong, Jake Varley, Alexander Herzog, Isabel Leal, Sean Kirmani, Dorsa Sadigh, Vikas Sindhwani, Kanishka Rao, Jacky Liang, and Andy Zeng. How to prompt your robot: A prompt-book for manipulation skills with code as policies. In *2nd Workshop on Language and Robot Learning: Language as Grounding*, 2023. URL <https://openreview.net/forum?id=T8AiZj1QdN>.

[3] Shikhar Bahl, Abhinav Gupta, and Deepak Pathak. Human-to-robot imitation in the wild. In *Robotics Science and Systems (RSS)*, 2022.

[4] Shikhar Bahl, Russell Mendonca, Lili Chen, Unnat Jain, and Deepak Pathak. Affordances from human videos as a versatile representation for robotics. In *Computer Vision and Pattern Recognition*, April 2023.

[5] Shikhar Bahl, Russell Mendonca, Lili Chen, Unnat Jain, and Deepak Pathak. Affordances from human videos as a versatile representation for robotics. In *Proceedings of the IEEE/CVF Conference on Computer Vision and Pattern Recognition*, pages 13778–13790, 2023.

[6] Yonatan Bisk, Rowan Zellers, Ronan Le Bras, Jianfeng Gao, and Yejin Choi. PIQA: Reasoning about Physical Commonsense in Natural Language. In *Thirty-Fourth AAAI Conference on Artificial Intelligence*, 2020. URL <https://yonatanbisk.com/piqa>.

[7] Konstantinos Bousmalis, Giulia Vezzani, Dushyant Rao, Coline Devin, Alex X. Lee, Maria Bauzá, Todor Davchev, Yuxiang Zhou, Agrim Gupta, Akhil S. Raju, Antoine Laurens, Claudio Fantacci, Valentin Dalibard, Martina

- Zambelli, Murilo Fernandes Martins, Rugile Pevcevičiute, Michiel Blokzijl, Misha Denil, Nathan Batchelor, Thomas Lampe, Emilio Parisotto, Konrad Zolna, Scott E. Reed, Sergio Gomez Colmenarejo, Jonathan Scholz, Abbas Abdolmaleki, Oliver Groth, Jean-Baptiste Regli, Oleg O. Sushkov, Tom Rothorl, José Enrique Chen, Yusuf Aytar, David Barker, Joy Ortiz, Martin A. Riedmiller, Jost Tobias Springenberg, Raia Hadsell, Francesco Nori, and Nicolas Manfred Otto Heess. Robocat: A self-improving generalist agent for robotic manipulation. In *Transactions on Machine Learning Research*, September 2023.
- [8] Anthony Brohan, Noah Brown, Justice Carbajal, Yevgen Chebotar, Joseph Dabis, Chelsea Finn, Keerthana Gopalakrishnan, Karol Hausman, Alex Herzog, Jasmine Hsu, Julian Ibarz, Brian Ichter, Alex Irpan, Tomas Jackson, Sally Jesmonth, Nikhil J Joshi, Ryan Julian, Dmitry Kalashnikov, Yuheng Kuang, Isabel Leal, Kuang-Huei Lee, Sergey Levine, Yao Lu, Utsav Malla, Deeksha Manjunath, Igor Mordatch, Ofir Nachum, Carolina Parada, Jodilyn Peralta, Emily Perez, Karl Pertsch, Jor-nell Quiambao, Kanishka Rao, Michael Ryoo, Grecia Salazar, Pannag Sanketi, Kevin Sayed, Jaspiar Singh, Sumedh Sontakke, Austin Stone, Clayton Tan, Huong Tran, Vincent Vanhoucke, Steve Vega, Quan Vuong, Fei Xia, Ted Xiao, Peng Xu, Sichun Xu, Tianhe Yu, and Brianna Zitkovich. RT-1: Robotics transformer for Real-World control at scale. In *arXiv preprint arXiv:2212.06817*, December 2022.
- [9] Anthony Brohan, Noah Brown, Justice Carbajal, Yevgen Chebotar, Xi Chen, Krzysztof Choromanski, Tianli Ding, Danny Driess, Avinava Dubey, Chelsea Finn, Pete Florence, Chuyuan Fu, Montse Gonzalez Arenas, Keerthana Gopalakrishnan, Kehang Han, Karol Hausman, Alex Herzog, Jasmine Hsu, Brian Ichter, Alex Irpan, Nikhil Joshi, Ryan Julian, Dmitry Kalashnikov, Yuheng Kuang, Isabel Leal, Lisa Lee, Tsang-Wei Edward Lee, Sergey Levine, Yao Lu, Henryk Michalewski, Igor Mordatch, Karl Pertsch, Kanishka Rao, Krista Reymann, Michael Ryoo, Grecia Salazar, Pannag Sanketi, Pierre Sermanet, Jaspiar Singh, Anikait Singh, Radu Soricut, Huong Tran, Vincent Vanhoucke, Quan Vuong, Ayzaan Wahid, Stefan Welker, Paul Wohlhart, Jialin Wu, Fei Xia, Ted Xiao, Peng Xu, Sichun Xu, Tianhe Yu, and Brianna Zitkovich. RT-2: Vision-Language-Action Models Transfer Web Knowledge to Robotic Control. In *arXiv preprint arXiv:2307.15818*, 2023.
- [10] Elliot Chane-Sane, Cordelia Schmid, and Ivan Laptev. Goal-conditioned reinforcement learning with imagined subgoals. In Marina Meila and Tong Zhang, editors, *Proceedings of the 38th International Conference on Machine Learning*, volume 139 of *Proceedings of Machine Learning Research*, pages 1430–1440. PMLR, 18–24 Jul 2021. URL <https://proceedings.mlr.press/v139/chane-sane21a.html>.
- [11] Ting Chen, Simon Kornblith, Kevin Swersky, Mohammad Norouzi, and Geoffrey E Hinton. Big self-supervised models are strong semi-supervised learners. *Advances in neural information processing systems*, 33: 22243–22255, 2020.
- [12] Sudeep Dasari and Abhinav Gupta. Transformers for one-shot visual imitation. In *Conference on Robot Learning*, pages 2071–2084. PMLR, 2021.
- [13] Eadom Dessalene, Chinmaya Devaraj, Michael Maynard, Cornelia Fermuller, and Yiannis Aloimonos. Forecasting action through contact representations from first person video. *IEEE Trans. Pattern Anal. Mach. Intell.*, 45(6): 6703–6714, June 2023.
- [14] Yiming Ding, Carlos Florensa, Mariano Phielipp, and Pieter Abbeel. Goal-conditioned imitation learning. In *Proceedings of the 33rd International Conference on Neural Information Processing Systems*, pages 15324–15335. Curran Associates Inc., Red Hook, NY, USA, December 2019.
- [15] Alexey Dosovitskiy, Lucas Beyer, Alexander Kolesnikov, Dirk Weissenborn, Xiaohua Zhai, Thomas Unterthiner, Mostafa Dehghani, Matthias Minderer, Georg Heigold, Sylvain Gelly, Jakob Uszkoreit, and Neil Houlsby. An image is worth 16x16 words: Transformers for image recognition at scale. In *International Conference on Learning Representations*, 2021. URL <https://openreview.net/forum?id=YicbFdNTTy>.
- [16] Yilun Du, Sherry Yang, Bo Dai, Hanjun Dai, Ofir Nachum, Joshua B. Tenenbaum, Dale Schuurmans, and Pieter Abbeel. Learning universal policies via text-guided video generation. In *Thirty-seventh Conference on Neural Information Processing Systems*, 2023. URL <https://openreview.net/forum?id=bo8q5MRcwY>.
- [17] Yan Duan, Marcin Andrychowicz, Bradly Stadie, OpenAI Jonathan Ho, Jonas Schneider, Ilya Sutskever, Pieter Abbeel, and Wojciech Zaremba. One-shot imitation learning. *Advances in neural information processing systems*, 30, 2017.
- [18] Debidatta Dwibedi, Yusuf Aytar, Jonathan Tompson, Pierre Sermanet, and Andrew Zisserman. Temporal Cycle-Consistency learning. In *Computer Vision and Pattern Recognition*, 2019.
- [19] Oliver Groth, Chia-Man Hung, Andrea Vedaldi, and Ingmar Posner. Goal-Conditioned End-to-End visuomotor control for versatile skill primitives. In *2021 IEEE International Conference on Robotics and Automation (ICRA)*, pages 1319–1325. IEEE, May 2021.
- [20] Andrew Jaegle, Sebastian Borgeaud, Jean-Baptiste Alayrac, Carl Doersch, Catalin Ionescu, David Ding, Skanda Koppula, Daniel Zoran, Andrew Brock, Evan Shelhamer, Olivier J Henaff, Matthew Botvinick, Andrew Zisserman, Oriol Vinyals, and Joao Carreira. Perceiver IO: A general architecture for structured inputs & outputs. In *International Conference on Learning Representations*, 2022. URL <https://openreview.net/forum?id=fILj7WpI-g>.
- [21] Vidhi Jain, Yixin Lin, Eric Undersander, Yonatan Bisk,

- and Akshara Rai. Transformers are adaptable task planners. In Karen Liu, Dana Kulic, and Jeff Ichnowski, editors, *Proceedings of The 6th Conference on Robot Learning*, volume 205 of *Proceedings of Machine Learning Research*, pages 1011–1037. PMLR, 14–18 Dec 2023. URL <https://proceedings.mlr.press/v205/jain23a.html>.
- [22] Eric Jang, Alex Irpan, Mohi Khansari, Daniel Kappler, Frederik Ebert, Corey Lynch, Sergey Levine, and Chelsea Finn. BC-Z: Zero-Shot Task Generalization with Robotic Imitation Learning. In *Proceedings of the 5th Conference on Robot Learning*, pages 991–1002, 2022.
- [23] Eric Jang, Alex Irpan, Mohi Khansari, Daniel Kappler, Frederik Ebert, Corey Lynch, Sergey Levine, and Chelsea Finn. Bc-z: Zero-shot task generalization with robotic imitation learning. In *Conference on Robot Learning*, pages 991–1002. PMLR, 2022.
- [24] Yunfan Jiang, Agrim Gupta, Zichen Zhang, Guanzhi Wang, Yongqiang Dou, Yanjun Chen, Li Fei-Fei, Anima Anandkumar, Yuke Zhu, and Linxi Fan. VIMA: General robot manipulation with multimodal prompts. In *Fortieth International Conference on Machine Learning*, 2023.
- [25] Jacob Krantz, Theophile Gervet, Karmesh Yadav, Austin Wang, Chris Paxton, Roozbeh Mottaghi, Dhruv Batra, Jitendra Malik, Stefan Lee, and Devendra Singh Chaplot. Navigating to objects specified by images. In *Proceedings of the IEEE/CVF International Conference on Computer Vision*, pages 10916–10925, 2023.
- [26] Sateesh Kumar, Jonathan Zamora, Nicklas Hansen, Rishabh Jangir, and Xiaolong Wang. Graph inverse reinforcement learning from diverse videos, 2022.
- [27] Jacky Liang, Wenlong Huang, Fei Xia, Peng Xu, Karol Hausman, Brian Ichter, Pete Florence, and Andy Zeng. Code as policies: Language model programs for embodied control. In *2023 IEEE International Conference on Robotics and Automation (ICRA)*, 2023.
- [28] Yuxuan Liu, Abhishek Gupta, Pieter Abbeel, and Sergey Levine. Imitation from observation: Learning to imitate behaviors from raw video via context translation. In *2018 IEEE International Conference on Robotics and Automation (ICRA)*, pages 1118–1125. IEEE, May 2018.
- [29] Yecheng Jason Ma, Shagun Sodhani, Dinesh Jayaraman, Osbert Bastani, Vikash Kumar, and Amy Zhang. VIP: Towards universal visual reward and representation via Value-Implicit Pre-Training. In *International Conference on Learning Representations*, 2023.
- [30] Zhao Mandi, Fangchen Liu, Kimin Lee, and Pieter Abbeel. Towards more generalizable one-shot visual imitation learning. In *2022 International Conference on Robotics and Automation (ICRA)*, pages 2434–2444. IEEE, 2022.
- [31] Russell Mendonca, Shikhar Bahl, and Deepak Pathak. Structured world models from human videos. In *RSS*, 2023.
- [32] Antoine Miech, Dimitri Zhukov, Jean-Baptiste Alayrac, Makarand Tapaswi, Ivan Laptev, and Josef Sivic. HowTo100M: Learning a Text-Video Embedding by Watching Hundred Million Narrated Video Clips. In *ICCV*, 2019.
- [33] Ashvin Nair, Vitchyr Pong, Murtaza Dalal, Shikhar Bahl, Steven Lin, and Sergey Levine. Visual reinforcement learning with imagined goals. In *NeurIPS*, July 2018.
- [34] Suraj Nair, Aravind Rajeswaran, Vikash Kumar, Chelsea Finn, and Abhinav Gupta. R3m: A universal visual representation for robot manipulation. In *6th Annual Conference on Robot Learning*, 2022. URL <https://openreview.net/forum?id=tGbpzg6yOrI>.
- [35] Open X-Embodiment Collaboration, Abhishek Padalkar, Acorn Pooley, Ajay Mandlekar, Ajinkya Jain, Albert Tung, Alex Bewley, Alex Herzog, Alex Irpan, Alexander Khazatsky, Anant Rai, Anikait Singh, Animesh Garg, Anthony Brohan, Antonin Raffin, Ayzaan Wahid, Ben Burgess-Limerick, Beomjoon Kim, Bernhard Schölkopf, Brian Ichter, Cewu Lu, Charles Xu, Chelsea Finn, Chenfeng Xu, Cheng Chi, Chenguang Huang, Christine Chan, Chuer Pan, Chuyuan Fu, Coline Devin, Danny Driess, Deepak Pathak, Dhruv Shah, Dieter Büchler, Dmitry Kalashnikov, Dorsa Sadigh, Edward Johns, Federico Ceola, Fei Xia, Freek Stulp, Gaoyue Zhou, Gaurav S Sukhatme, Gautam Salhotra, Ge Yan, Giulio Schiavi, Gregory Kahn, Hao Su, Hao-Shu Fang, Haochen Shi, Heni Ben Amor, Henrik I Christensen, Hiroki Furuta, Homer Walke, Hongjie Fang, Igor Mordatch, Ilija Radosavovic, Isabel Leal, Jacky Liang, Jad Abou-Chakra, Jaehyung Kim, Jan Peters, Jan Schneider, Jasmine Hsu, Jeannette Bohg, Jeffrey Bingham, Jiajun Wu, Jialin Wu, Jianlan Luo, Jiayuan Gu, Jie Tan, Jihoon Oh, Jitendra Malik, Jonathan Booher, Jonathan Tompson, Jonathan Yang, Joseph J Lim, João Silvério, Junhyek Han, Kanishka Rao, Karl Pertsch, Karol Hausman, Keegan Go, Keerthana Gopalakrishnan, Ken Goldberg, Kendra Byrne, Kenneth Oslund, Kento Kawaharazuka, Kevin Zhang, Krishan Rana, Krishnan Srinivasan, Lawrence Yunliang Chen, Lerrel Pinto, Li Fei-Fei, Liam Tan, Lionel Ott, Lisa Lee, Masayoshi Tomizuka, Max Spero, Maximilian Du, Michael Ahn, Mingtong Zhang, Mingyu Ding, Mohan Kumar Srirama, Mohit Sharma, Moo Jin Kim, Naoaki Kanazawa, Nicklas Hansen, Nicolas Heess, Nikhil J Joshi, Niko Suenderhauf, Norman Di Palo, Nur Muhammad Mahi Shafiullah, Oier Mees, Oliver Kroemer, Pannag R Sanketi, Paul Wohlhart, Peng Xu, Pierre Sermanet, Priya Sundaresan, Quan Vuong, Rafael Rafailov, Ran Tian, Ria Doshi, Roberto Martín-Martín, Russell Mendonca, Rutav Shah, Ryan Hoque, Ryan Julian, Samuel Bustamante, Sean Kirmani, Sergey Levine, Sherry Moore, Shikhar Bahl, Shivin Dass, Shubham Sonawani, Shuran Song, Sichun Xu, Siddhant Haldar, Simeon Adebola, Simon Guist, Soroush Nasiriany, Stefan Schaal, Stefan Welker, Stephen Tian, Sudeep Dasari, Suneel Belkhale, Takayuki Osa, Tatsuya Harada, Tatsuya Matsushima, Ted Xiao, Tianhe Yu, Tianli Ding, Todor Davchev, Tony Z Zhao, Travis Armstrong, Trevor Darrell, Vidhi Jain, Vincent Van-

- houcke, Wei Zhan, Wenxuan Zhou, Wolfram Burgard, Xi Chen, Xiaolong Wang, Xinghao Zhu, Xuanlin Li, Yao Lu, Yevgen Chebotar, Yifan Zhou, Yifeng Zhu, Ying Xu, Yixuan Wang, Yonatan Bisk, Yoonyoung Cho, Youngwoon Lee, Yuchen Cui, Yueh-Hua Wu, Yujin Tang, Yuke Zhu, Yunzhu Li, Yusuke Iwasawa, Yutaka Matsuo, Zhuo Xu, and Zichen Jeff Cui. Open X-Embodiment: Robotic learning datasets and RT-X models. *arXiv preprint arXiv:2310.08864*, 2023.
- [36] Priyam Parashar, Vidhi Jain, Xiaohan Zhang, Jay Vakil, Sam Powers, Yonatan Bisk, and Chris Paxton. Spatial-Language Attention Policies for Efficient Robot Learning. In *Conference on Robot Learning*, 2023. URL <https://arxiv.org/abs/2304.11235>.
- [37] Xue Bin Peng, Angjoo Kanazawa, Jitendra Malik, Pieter Abbeel, and Sergey Levine. SFV: reinforcement learning of physical skills from videos. *ACM Trans. Graph.*, 37(6):1–14, December 2018.
- [38] Ethan Perez, Florian Strub, Harm De Vries, Vincent Dumoulin, and Aaron Courville. Film: Visual reasoning with a general conditioning layer. In *Proceedings of the AAAI conference on artificial intelligence*, 2018.
- [39] Vladimír Petrík, Makarand Tapaswi, Ivan Laptev, and Josef Sivic. Learning object manipulation skills via approximate state estimation from real videos. In Jens Kober, Fabio Ramos, and Claire Tomlin, editors, *Proceedings of the 2020 Conference on Robot Learning*, volume 155 of *Proceedings of Machine Learning Research*, pages 296–312. PMLR, 2021.
- [40] Sören Pirk, Mohi Khansari, Yunfei Bai, Corey Lynch, and Pierre Sermanet. Online learning of object representations by appearance space feature alignment. In *2020 IEEE International Conference on Robotics and Automation (ICRA)*, pages 10473–10479, 2020. doi: 10.1109/ICRA40945.2020.9196567.
- [41] Karl Schmeckpeper, Oleh Rybkin, Kostas Daniilidis, Sergey Levine, and Chelsea Finn. Reinforcement learning with videos: Combining offline observations with interaction. *arXiv preprint arXiv:2011.06507*, 2020.
- [42] Rutav Shah, Roberto Martín-Martín, and Yuke Zhu. MUTEX: Learning unified policies from multimodal task specifications. In *7th Annual Conference on Robot Learning*, 2023.
- [43] Pratyusha Sharma, Deepak Pathak, and Abhinav Gupta. Third-Person visual imitation learning via decoupled hierarchical controller. *Adv. Neural Inf. Process. Syst.*, 32, 2019.
- [44] Laura Smith, Nikita Dhawan, Marvin Zhang, Pieter Abbeel, and Sergey Levine. AVID: Learning Multi-Stage tasks via Pixel-Level translation of human videos. In *Robotics: Science and Systems (RSS)*, December 2020.
- [45] Austin Stone, Ted Xiao, Yao Lu, Keerthana Gopalakrishnan, Kuang-Huei Lee, Quan Vuong, Paul Wohlhart, Sean Kirmani, Brianna Zitkovich, Fei Xia, Chelsea Finn, and Karol Hausman. Open-World object manipulation using pre-trained Vision-Language models. In *Conference on Robot Learning*, March 2023.
- [46] Chen Wang, Linxi Fan, Jiankai Sun, Ruohan Zhang, Li Fei-Fei, Danfei Xu, Yuke Zhu, and Anima Anandkumar. Mimicplay: Long-horizon imitation learning by watching human play. *arXiv preprint arXiv:2302.12422*, 2023.
- [47] Tete Xiao, Ilija Radosavovic, Trevor Darrell, and Jitendra Malik. Masked visual pre-training for motor control. *arXiv preprint arXiv:2203.06173*, 2023.
- [48] Mengda Xu, Zhenjia Xu, Cheng Chi, Manuela Veloso, and Shuran Song. XSkill: Cross embodiment skill discovery. In *7th Annual Conference on Robot Learning*, 2023. URL <https://openreview.net/forum?id=8L6pHd9aS6w>.
- [49] Sriram Yenamandra, Arun Ramachandran, Karmesh Yadav, Austin Wang, Mukul Khanna, Theophile Gervet, Tsung-Yen Yang, Vidhi Jain, Alexander William Clegg, John Turner, Zsolt Kira, Manolis Savva, Angel Chang, Devendra Singh Chaplot, Dhruv Batra, Roozbeh Motlaghi, Yonatan Bisk, and Chris Paxton. HomeRobot: Open-Vocabulary Mobile Manipulation. In *Conference on Robot Learning*, 2023. URL <https://arxiv.org/abs/2306.11565>.
- [50] Jiahui Yu, Zirui Wang, Vijay Vasudevan, Legg Yeung, Mojtaba Seyedhosseini, and Yonghui Wu. Coca: Contrastive captioners are image-text foundation models. *arXiv preprint arXiv:2205.01917*, 2022.
- [51] Kevin Zakka, Andy Zeng, Pete Florence, Jonathan Tompson, Jeannette Bohg, and Debidatta Dwibedi. Xirl: Cross-embodiment inverse reinforcement learning. In *Conference on Robot Learning*, pages 537–546. PMLR, 2022.
- [52] Xiaohua Zhai, Basil Mustafa, Alexander Kolesnikov, and Lucas Beyer. Sigmoid loss for language image pre-training. In *2023 IEEE/CVF International Conference on Computer Vision (ICCV)*, pages 11941–11952, Los Alamitos, CA, USA, oct 2023. IEEE Computer Society. doi: 10.1109/ICCV51070.2023.01100.
- [53] Tony Z Zhao, Vikash Kumar, Sergey Levine, and Chelsea Finn. Learning Fine-Grained bimanual manipulation with Low-Cost hardware. In *Robotics: Science and Systems*, 2023.